Wuhan University
Journal of Natural Sciences

2022, Vol.27 No.2, 142-152

Article ID 1007-1202(2022)02-0142-11
DOI https://doi.org/10.1051/wujns/2022272142

Optimal Power Flow Calculation of Active Distribution Network Based on Improved Comprehensive Technology

☐ CAO Hongji[1,2], LIU Daobing[1,2†], LI Shichun[1,2], JIN Zitong[1,2], YUAN Ye[1,2], XU Songlin[1,2]

1. College of Electrical Engineering and New Energy, China Three Gorges University, Yichang 443002, Hubei, China;

2. Hubei Provincial Key Laboratory for Operation and Control of Cascade Hydropower Station, China Three Gorges University, Yichang 443002, Hubei, China

Abstract: Comprehensive unified power flow controller (UPFC) technology can calculate voltage control parameters of UPFC, but it increases the nonlinearity of Newton power flow calculation. When the comprehensive technology is combined with the intelligent algorithm, the control parameters can only be optimized through the active and reactive power of UPFC on the branch, which makes the optimization convergence worse. Therefore, an optimal power flow calculation method for active distribution network based on improved comprehensive technology is proposed. First, based on the analysis of the influence of UPFC on branch power flow, an improved UPFC model is proposed. The accuracy of UPFC control parameters is enhanced by adjusting the voltage phase angle and regulation radius of series side transformer. Second, the optimal control model considering UPFC is established. Finally, the corresponding self-admittance and mutual admittance elements are extracted from the constructed UPFC model and introduced into the Jacobian matrix, so that while the comprehensive technology maintains the dimension of the Jacobian matrix, the intelligent algorithm can directly optimize the control parameters to reduce the search space. The IEEE33 bus system is used for example simulation, the results before and after the improvement are compared, and the Monte Carlo method is used to calculate the two algorithms 50 times respectively based on the installation number of UPFC, which verifies that the proposed optimization method has better convergence and operation speed.

Key words: unified power flow controller (UPFC); active distribution network; power flow calculation; optimal power flow; Jacobian matrix; comprehensive UPFC technique

CLC number: TM 732

Received date: 2021-11-05
Foundation item: Supported by the National Natural Science Foundation of China (51907104)
Biography: CAO Hongji, male, Master candidate, research direction: active distribution network operation optimization. E-mail: 349082828@qq.com
† To whom correspondence should be addressed. E-mail: liudb@ctgu.edu.cn

0 Introduction

The access of distributed generation is an important measure for the development of China's power industry[1], which poses new challenges to the planning and operation of traditional distribution network, and promotes the transformation of traditional passive distribution network to active distribution network (ADN) with power flow active control capability and load interaction capability[2,3]. The complex network structure of distribution network makes the network overcrowded, which often leads to serious congestion[4]. In addition, only relying on the improvement of network topology is not enough to absorb a large number of distributed generators, so it is necessary to increase the controllable equipment and resources of distribution network[5]. Therefore, unified power flow controller (UPFC) is introduced to meet the construction requirements of new distribution network. UPFC has the functions of voltage regulation, phase shift, impedance compensation, integrated control and other functions[6,7]. Giving full play to the regulation ability of UPFC can improve the safety and economy of power grid operation[8,9]. Therefore, the research on ADN power flow optimization with UPFC is of great significance.

Ref.[10] used the equivalent power injection model to optimize the control of distribution network. Refs. [11-13] coordinated control of node voltage and network loss of distribution ring network through UPFC. The above research is the application of the control strategy of the new UPFC. The power at both ends is equivalent to the node injection power without changing the power flow and branch current model. However, the series and parallel sides of the traditional UPFC are connected at

the same node, so it is necessary to establish a new optimal control model considering the traditional UPFC.

UPFC is one of the most important flexible alternating current (AC) transmission system equipment. Embedding flexible AC transmission system devices in power flow algorithm is regarded as the basic requirement of planning, operation and control. Generally, it is necessary to modify the existing power flow program to include these equipment. However, the equivalent model of UPFC is not modeled based on the actual circuit, resulting in a certain gap between the analysis results and the actual situation[14]. Comprehensive UPFC technology[15] is a unified method to connect AC network and UPFC state variables in the same equation, which can calculate the control voltage, active power and reactive power of UPFC, and then reflect the real parameters of the original actual circuit, but the Jacobian matrix dimension increases according to the number of UPFC, resulting in poor convergence and slow operation speed. The latest relevant research literature [16] introduces UPFC into the power flow equation, but still adds the dimension of Jacobian matrix. In addition, the combination of comprehensive technology and intelligent algorithm has certain defects: the comprehensive technology increases the nonlinearity of Newton power flow calculation, and the active and reactive power of nodes associated with UPFC need to be corrected in the iterative process[17], and the convergence of the system becomes worse. The intelligent algorithm cannot retain the better UPFC control value for the next round of iteration, and the initial value of UPFC control is always the fixed value, which needs to be further improved. The UPFC parameters need to be optimized in the optimization control. If the voltage amplitude and phase angle of the UPFC are solved by the intelligent algorithm to replace the active and reactive variables of the UPFC on the branch, the search space can be reduced. In addition, if the self-admittance and mutual admittance elements generated by the UPFC are introduced into the Jacobian matrix, there is no need to add the dimension of Newton power flow algorithm and modify the active and reactive power of the nodes associated with UPFC in the process of power flow calculation. With the increase of the number of iterations of the intelligent algorithm, the initial value of UPFC of each optimized individual will be closer and closer to the better value. The convergence speed and effect of power flow calculation are expected to be improved.

To solve the above problems, an ADN optimal power flow calculation method based on improved comprehensive technology is proposed in this paper. First, the influence of UPFC on branch power flow is analyzed: the power generated by its voltage on the branch can be extracted and modeled separately. On this basis, in order to separate the UPFC equation from Newton power flow calculation, the UPFC model is improved by adding the voltage phase angle and regulation radius variable of series side transformer. Second, the ADN optimal control model considering UPFC is established. Finally, the self-admittance and mutual admittance elements generated by UPFC are introduced into the Jacobian matrix, so that while the comprehensive technology maintains the dimension of the Jacobian matrix, the intelligent algorithm can directly optimize the control parameters based on the comprehensive technology to reduce the search space. An example is given to verify the effectiveness of the model.

1 UPFC Model

One voltage source converter (VSC) of UPFC is connected in series in AC line through transformer, the other VSC is connected in parallel to the node through transformer, and the two VSCs are connected through direct current (DC) bus capacitance[18]. The structure of UPFC proposed in this paper is shown in Fig. 1. The UPFC is installed on the ADN line. While changing the power flow of the line through series side and parallel side transformers, it can also provide or absorb reactive power.

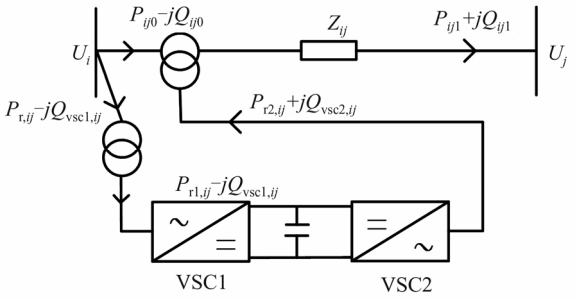

Fig.1 UPFC model structure

For the convenience of modeling, it is assumed that the node of ADN connected to the main network is the root node, and UPFC is only installed on the parent node side of each branch. P_{ij0} and Q_{ij0} are respectively the active and reactive power generated by UPFC on the node i side of branch ij. P_{ij1} and Q_{ij1} are respectively the active and reactive power generated by UPFC on the node j side of branch ij. $P_{r,ij}$ is the active power injected into the transformer on the parallel side of UPFC on the node i

side of branch *ij*. $P_{r1,ij}$ is the active power of VSC1 injected into UPFC on branch *ij*. $P_{r2,ij}$ is the active power output by VSC2 of UPFC on branch *ij*. $Q_{VSC1,ij}$ and $Q_{VSC2,ij}$ are the reactive power of VSC1 and VSC2 of UPFC on branch *ij*, respectively. Z_{ij} is the impedance of line *ij*. U_i and U_j are the voltage of nodes *i* and *j*, respectively. The ground admittance can be ignored in ADN operation optimization calculation[19]. Therefore, the ground admittance of UPFC power model on the line in Ref. [20] can be ignored. On this basis, in order to facilitate Newton power flow calculation, the power model of UPFC on the line is improved. The power model generated by UPFC on the line after ignoring the ground admittance:

$$P_{ij0} = U_i U_{ij}(g_{ij}\cos\theta_{i,ij} + b_{ij}\sin\theta_{i,ij}) \tag{1}$$

$$Q_{ij0} = U_i U_{ij}(g_{ij}\sin\theta_{i,ij} - b_{ij}\cos\theta_{i,ij}) \tag{2}$$

$$P_{ij1} = U_j U_{ij}(g_{ij}\cos\theta_{j,ij} + b_{ij}\sin\theta_{j,ij}) \tag{3}$$

$$Q_{ij1} = U_j U_{ij}(g_{ij}\sin\theta_{j,ij} - b_{ij}\cos\theta_{j,ij}) \tag{4}$$

where $\theta_{i,ij}$ is the difference between the voltage phase angle of node *i* and the equivalent voltage phase angle on the series side of branch *ij*, g_{ij} and b_{ij} are the conductance and susceptance of line *ij*, respectively, and U_{ij} is the voltage amplitude of the equivalent voltage source at the series side of UPFC of branch *ij*. In order to improve the power flow algorithm, constraints (5)-(7) are introduced:

$$U_{ij} = r_{ij}U_i \tag{5}$$

$$0 \le r_{ij} \le r_{ij,\max} \tag{6}$$

$$0 \le \rho_{ij} \le 2\pi \tag{7}$$

where r_{ij} is the UPFC voltage regulation radius of branch *ij*, $r_{ij,\max}$ is the maximum UPFC voltage regulation radius of branch *ij*, and ρ_{ij} is the voltage phase difference between the equivalent voltage source on the UPFC series side of branch *ij* and node *i*. Then:

$$\theta_{j,ij} = \theta_j - \theta_i - \rho_{ij} \tag{8}$$

where θ_i is the voltage phase angle of node *i*. Substituting equations (5) and (8) into equations (1) to (4):

$$P_{ij0} = U_i U_{ij}[g_{ij}\cos(\theta_i - \theta_i - \rho_{ij}) + b_{ij}\sin(\theta_i - \theta_i - \rho_{ij})] \tag{9}$$

$$Q_{ij0} = U_i U_{ij}[g_{ij}\sin(\theta_i - \theta_i - \rho_{ij}) - b_{ij}\cos(\theta_i - \theta_i - \rho_{ij})] \tag{10}$$

$$P_{ij1} = U_j U_{ij}[g_{ij}\cos(\theta_j - \theta_i - \rho_{ij}) + b_{ij}\sin(\theta_j - \theta_i - \rho_{ij})] \tag{11}$$

$$Q_{ij1} = U_j U_{ij}[g_{ij}\sin(\theta_j - \theta_i - \rho_{ij}) - b_{ij}\cos(\theta_j - \theta_i - \rho_{ij})] \tag{12}$$

The improved power model of UPFC is obtained:

$$P_{ij0} = U_i U_{ij}[g_{ij}\cos\rho_{ij} - b_{ij}\sin\rho_{ij}] \tag{13}$$

$$Q_{ij0} = U_i U_{ij}[-g_{ij}\sin\rho_{ij} - b_{ij}\cos\rho_{ij}] \tag{14}$$

$$P_{ij1} = U_j U_{ij}[g_{ij}\cos(\theta_{ij} + \rho_{ij}) - b_{ij}\sin(\theta_{ij} + \rho_{ij})] \tag{15}$$

$$Q_{ij1} = U_j U_{ij}[-g_{ij}\sin(\theta_{ij} + \rho_{ij}) - b_{ij}\cos(\theta_{ij} + \rho_{ij})] \tag{16}$$

where θ_{ij} is the voltage phase angle difference of line *ij*. Power balance equation of UPFC series side transformer:

$$P_{r2,ij} - P_{TL2,ij} = P_{ij1} - P_{ij0} \tag{17}$$

$$Q_{VSC2,ij} = Q_{ij1} - Q_{ij0} \tag{18}$$

where $P_{TL2,ij}$ is the loss of UPFC series side transformer on branch *ij*. Active power balance equation of UPFC parallel side transformer:

$$P_{r,ij} - P_{TL1,ij} = P_{r1,ij} \tag{19}$$

where $P_{TL1,ij}$ is the transformer losses at the parallel side of UPFC on branch *ij*. Transformer losses include variable losses and fixed losses:

$$P_{TL1,ij} = [(P_{r,ij}^2 + Q_{VSC1,ij}^2)/U_i^2]R_{TL1,ij} + (U_i/U_{e1,ij})P_{0T1,ij} \tag{20}$$

$$P_{TL2,ij} = [(P_{r2,ij}^2 + Q_{VSC2,ij}^2)/(U_{ij}k_{Tij})^2]R_{TL2,ij} + P_{0T2,ij}U_{ij}k_{Tij}/U_{e2,ij} \tag{21}$$

where $R_{TL1,ij}$, $U_{e1,ij}$ and $P_{0T1,ij}$ are the equivalent resistance, rated voltage and no-load loss of UPFC parallel side transformer on branch *ij* , respectively. $R_{TL2,ij}$, $U_{e2,ij}$ and $P_{0T2,ij}$ are the equivalent resistance, rated voltage and no-load loss of the UPFC series side transformer on branch *ij* respectively, and k_{Tij} is the voltage ratio between the valve side and the grid side of the UPFC series side transformer on branch *ij*. Active power balance equation of two VSCs:

$$P_{r1,ij} - P_{V1,ij} - P_{V2,ij} = P_{r2,ij} \tag{22}$$

where $P_{V1,ij}$ and $P_{V2,ij}$ are the losses of VSC1 and VSC2 of UPFC on branch *ij*, respectively. There will be a certain loss of electric energy transmitted through VSC [21]:

$$P_{V1,ij} = A_{V1,ij}\sqrt{P_{r1,ij}^2 + Q_{VSC1,ij}^2} \tag{23}$$

$$P_{V2,ij} = A_{V2,ij}\sqrt{P_{r2,ij}^2 + Q_{VSC2,ij}^2} \tag{24}$$

where $A_{V1,ij}$ and $A_{V2,ij}$ are the loss coefficients of VSC1 and VSC2 of UPFC on branch *ij* , respectively. VSC capacity is determined by the active and reactive power flowing through, and its constraints are as follows:

$$\sqrt{P_{r1,ij}^2 + Q_{VSC1,ij}^2} \le S_{VSC1,ij}^{\max} \tag{25}$$

$$\sqrt{P_{r2,ij}^2 + Q_{VSC2,ij}^2} \le S_{VSC2,ij}^{\max} \tag{26}$$

$$Q_{VSC1,ij}^{\min} \le Q_{VSC1,ij} \le Q_{VSC1,ij}^{\max} \tag{27}$$

$$Q_{VSC2,ij}^{\min} \le Q_{VSC2,ij} \le Q_{VSC2,ij}^{\max} \tag{28}$$

where $S_{VSC1,ij}^{\max}$ and $S_{VSC2,ij}^{\max}$ are the maximum capacity of VSC1 and VSC2 of branch *ij* , respectively. $Q_{VSC1,ij}^{\min}$ and $Q_{VSC1,ij}^{\max}$ are the minimum and maximum reactive

power generated by VSC1 of branch ij , respectively. $Q_{\mathrm{VSC2},ij}^{\min}$ and $Q_{\mathrm{VSC2},ij}^{\max}$ are the minimum and maximum reactive power generated by VSC2 of branch ij , respectively.

2 Optimization Control Strategy

2.1 Objective Function

Considering that the reduced output price of clean energy is greater than the power sale price, it is generally based on the maximum power output, which is not suitable to be used as scheduling resources to optimize the network loss to highlight the role of UPFC. Therefore, only micro-turbine (MT) is considered in the distributed power supply in this paper. The operation cost includes network loss, interaction with superior power grid, demand response, MT power generation and UPFC loss cost.

$$\min C = C_{\mathrm{loss}} + C_{\mathrm{P0}} + C_{\mathrm{DSR}} + C_{\mathrm{MT}} + C_{\mathrm{UPFC}} \tag{29}$$

where C is the objective function of the optimization control strategy, C_{loss} is the network loss cost, C_{P0} is the interaction cost with the superior power grid, C_{DSR} is the demand response cost, C_{MT} is the MT power generation cost, and C_{UPFC} is the loss cost of UPFC.

1) Network loss

$$C_{\mathrm{loss}} = \omega \sum_{ij \in E} l_{ij} R_{ij} t^{\Delta} \tag{30}$$

where l_{ij} is the square of branch ij current, R_{ij} is the resistance of branch ij, ω is the electricity selling price constant, E is the ADN line set, and t^{Δ} is the length of the period.

2) Interaction cost with superior power grid

$$C_{\mathrm{P0}} = \lambda_{\mathrm{P0}} \sum_{i=1}^{i=N} P_{0i} t^{\Delta} \tag{31}$$

where λ_{P0} is the price constant of unit power of interaction between ADN and superior power grid, P_{0i} is the active power of interaction between node i and superior power grid, and N is the number of network nodes of ADN.

3) Demand response side cost

$$C_{\mathrm{DSR}} = \lambda_{\mathrm{CUT}} \sum_{i=1}^{i=N} P_{\mathrm{CUT}i} t^{\Delta} \tag{32}$$

where λ_{CUT} is the price constant of load reduction, and $P_{\mathrm{CUT}i}$ is the load reduction of node i.

4) MT power generation cost

MT power generation cost includes fuel[22] and VSC loss cost:

$$C_{\mathrm{MT}} = \sum_{i=1}^{i=N} [\lambda_{\mathrm{MT}} P_{\mathrm{MT}i} + \omega (P_{\mathrm{MTV1}i} + P_{\mathrm{MTV2}i})] t^{\Delta} \tag{33}$$

where λ_{MT} is the fuel cost of MT unit power generation, $P_{\mathrm{MTV1}i}$ and $P_{\mathrm{MTV2}i}$ are the loss of VSC at MT side and network side of node i , respectively, and $P_{\mathrm{MT}i}$ is the active power of MT at node i.

5) UPFC loss cost

UPFC losses include transformer and VSC losses:

$$C_{\mathrm{UPFC}} = \omega \sum_{ij \in E} (P_{\mathrm{TL1},ij} + P_{\mathrm{TL2},ij} + P_{\mathrm{V1},ij} + P_{\mathrm{V2},ij}) t^{\Delta} \tag{34}$$

2.2 Constraints

1) MT constraint

Due to the single period optimization, the time series coupling characteristics of MT active output are not considered, and only the upper and lower limits are limited. The constraints are as follows:

$$P_{\mathrm{MT}i,\min} \le P_{\mathrm{MT}i} \le P_{\mathrm{MT}i,\max} \tag{35}$$

$$\sqrt{P_{\mathrm{MT}i}^2 + Q_{\mathrm{MT}i}^2} \le S_{\mathrm{MT}i}^{\max} \tag{36}$$

where $P_{\mathrm{MT}i,\min}$ is the lower limit of active output of MT at node i, $P_{\mathrm{MT}i,\max}$ is the upper limit of active output of MT at node i, $Q_{\mathrm{MT}i}$ is the reactive power of MT at node i, and $S_{\mathrm{MT}i}^{\max}$ is the apparent power of MT at node i. MT power network access needs to go through VSC[23], and its structure is shown in Fig. 2.

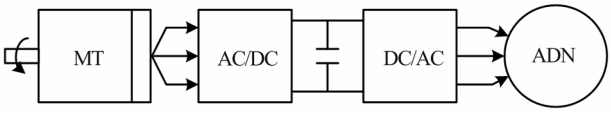

Fig. 2 Connection structure of MT and network

VSC loss:

$$P_{\mathrm{MTV1}i} = A_{\mathrm{MT},i} \sqrt{P_{\mathrm{MT}i}^2 + Q_{\mathrm{MT}i}^2} \tag{37}$$

$$P_{\mathrm{MTV2}i} = A_{\mathrm{MT},i} \sqrt{P_{\mathrm{MTG}i}^2 + Q_{\mathrm{MT}i}^2} \tag{38}$$

where $P_{\mathrm{MTG}i}$ is the active power injected into the network by MT at node i, and $A_{\mathrm{MT},i}$ is the VSC loss coefficient of MT at node i. Network access power balance equation:

$$P_{\mathrm{MT}i} - P_{\mathrm{MTV1}i} - P_{\mathrm{MTV2}i} = P_{\mathrm{MTG}i} \tag{39}$$

In addition, it also contains VSC capacity constraints. It is assumed that VSC capacity is greater than MT capacity.

2) Node injection power constraint

$$P_i = P_{\mathrm{MTG}i} + P_{0i} - P_{\mathrm{L}i} + P_{\mathrm{CUT}i} - \sum_{j \in N(i)} P_{\mathrm{r},ij} \tag{40}$$

$$Q_i = Q_{\mathrm{MT}i} + Q_{0i} - Q_{\mathrm{L}i} + \sum_{j \in N(i)} Q_{\mathrm{VSC1},ij} \tag{41}$$

where P_i and Q_i are the active and reactive power injected from node i , respectively, Q_{0i} is the reactive power of node i interacting with the superior power grid, $P_{\mathrm{L}i}$ and $Q_{\mathrm{L}i}$ are the active and reactive loads of node i ,

respectively, and $N(i)$ is the set of sub nodes of node i.

3) Power balance constraint

$$\sum_{i=1}^{N}(P_{\mathrm{MTG}i}+P_{0i}-P_{\mathrm{L}i}+P_{\mathrm{CUT}i})-\sum_{ij\in E}(l_{ij}R_{ij}+P_{\mathrm{TL1},ij}+P_{\mathrm{TL2},ij}+P_{\mathrm{V1},ij}+P_{\mathrm{V2},ij})=0 \quad (42)$$

$$\sum_{i=1}^{N}(Q_{\mathrm{MT}i}+Q_{0i}-Q_{\mathrm{L}i})+\sum_{ij\in E}(Q_{\mathrm{VSC1},ij}+Q_{\mathrm{VSC2},ij}-l_{ij}X_{ij})=0 \quad (43)$$

where X_{ij} is the reactance of branch ij.

4) Node voltage constraint

$$U_{\min}\le U_i\le U_{\max} \quad (44)$$

$U_{\max}$ and $U_{\min}$ are the maximum and minimum values of node voltage, respectively.

5) Power flow constraint

The series side voltage of UPFC affects the branch power flow. Considering the power flow equation of UPFC:

$$\begin{cases} P_i=G_{ii}U_i^2+U_i\sum\limits_{j\in\Omega(i)}U_j(G_{ij}\cos\theta_{ij}+B_{ij}\sin\theta_{ij}) \\ \qquad +\sum\limits_{j\in N(i)}P_{ij0}-\sum\limits_{j\in M(i)}P_{ji1} \\ Q_i=-B_{ii}U_i^2+U_i\sum\limits_{j\in\Omega(i)}U_j(G_{ij}\sin\theta_{ij}-B_{ij}\cos\theta_{ij}) \\ \qquad +\sum\limits_{j\in N(i)}Q_{ij0}-\sum\limits_{j\in M(i)}Q_{ji1} \end{cases} \quad (45)$$

where G_{ij} and B_{ij} are mutual conductance and mutual susceptance between node i and node j , respectively, $M(i)$ is the parent node set of node i, and $\Omega(i)$ is the line set connected to node i.

6) Branch current constraint

Branch current constraint without UPFC[24]:

$$l_{ij}=(g_{ij}^2+b_{ij}^2)(U_i^2+U_j^2-2U_iU_j\cos\theta_{ij})\le I_{ij,\max}^2 \quad (46)$$

where $I_{ij,\max}$ is the maximum current of branch ij. Branch current for installing traditional UPFC:

$$l_{ij}=\left|g_{ij}+jb_{ij}\right|^2(\boldsymbol{U}_i+\boldsymbol{U}_{ij}-\boldsymbol{U}_j)^2\le I_{ij,\max}^2 \quad (47)$$

where $\boldsymbol{U}_i$ and $\boldsymbol{U}_j$ are the voltage phasor of nodes i and j, respectively, and $\boldsymbol{U}_{ij}$ is the voltage phasor of the equivalent voltage source at the series side of the UPFC of line ij. Expand equation (47):

$$l_{ij}=(g_{ij}^2+b_{ij}^2)(\boldsymbol{U}_i^2+\boldsymbol{U}_{ij}^2+\boldsymbol{U}_j^2+2\boldsymbol{U}_i\boldsymbol{U}_{ij}-2\boldsymbol{U}_i\boldsymbol{U}_j-2\boldsymbol{U}_{ij}\boldsymbol{U}_j)\le I_{ij,\max}^2 \quad (48)$$

The phasor is represented by amplitude and phase:

$$l_{ij}=(g_{ij}^2+b_{ij}^2)[U_i^2+U_{ij}^2+U_j^2-2U_iU_j\cos\theta_{ij}+2U_iU_{ij}\cos\rho_{ij}-2U_jU_{ij}\cos(\rho_{ij}+\theta_{ij})]\le I_{ij,\max}^2 \quad (49)$$

7) Load reduction, interactive power constraints with superior power grid

Ref. [25] introduces load reduction and interactive power constraints with superior power grid. Demand response load reduction constraints:

$$0\le P_{\mathrm{CUT}i}\le P_{\mathrm{CUT}i,\max} \quad (50)$$

where $P_{\mathrm{CUT}i,\max}$ is the maximum active power reduction of the controllable load of node i. In order to limit the impact of ADN on the superior power grid, there are certain constraints on their interactive power:

$$0\le P_{0i}\le P_{0i,\max} \quad (51)$$

$$0\le Q_{0i}\le Q_{0i,\max} \quad (52)$$

where $P_{0i,\max}$ and $Q_{0i,\max}$ are the upper limits of active and reactive power of interaction between node i of ADN and superior power grid , respectively.

8) UPFC constraints

Same as (5)-(7), (13)-(28).

3 Model Solution

3.1 Optimal Power Flow Calculation Based on Comprehensive UPFC Technology

In the optimization process, it is necessary to determine the active and reactive power generated by UPFC at the child node side firstly, and solve the voltage amplitude and phase angle of UPFC through comprehensive technology, which can be described as solving the following equations[26]:

$$F(\boldsymbol{X},\boldsymbol{X}_u)=0 \quad (53)$$

$$R(\boldsymbol{X},\boldsymbol{X}_u)=0 \quad (54)$$

where $\boldsymbol{X}$ is the state vector of the traditional power flow equation including node voltage amplitude and phase angle, and $\boldsymbol{X}_u$ is the state vector including UPFC injection voltage and phase angle. Equations (53) are node power balance equations considering UPFC. Equations (54) are governing equations and constraint equations with UPFC. Equations (54) and variable $\boldsymbol{X}_u$ increase the nonlinearity of Newton power flow calculation. In addition, the intelligent algorithm can only optimize $\boldsymbol{X}_u$ through the active and reactive power of UPFC on the branch, and the search space of active and reactive power is much larger than the voltage regulation radius and phase angle. The convergence of the system needs to be improved. The specific flow of optimal power flow calculation based on comprehensive technology is shown in Fig. 3.

3.2 Optimal Power Flow Calculation Based on Improved Comprehensive UPFC Technology

The optimal control model in this paper is a multivariable and multi-constraint nonlinear optimization

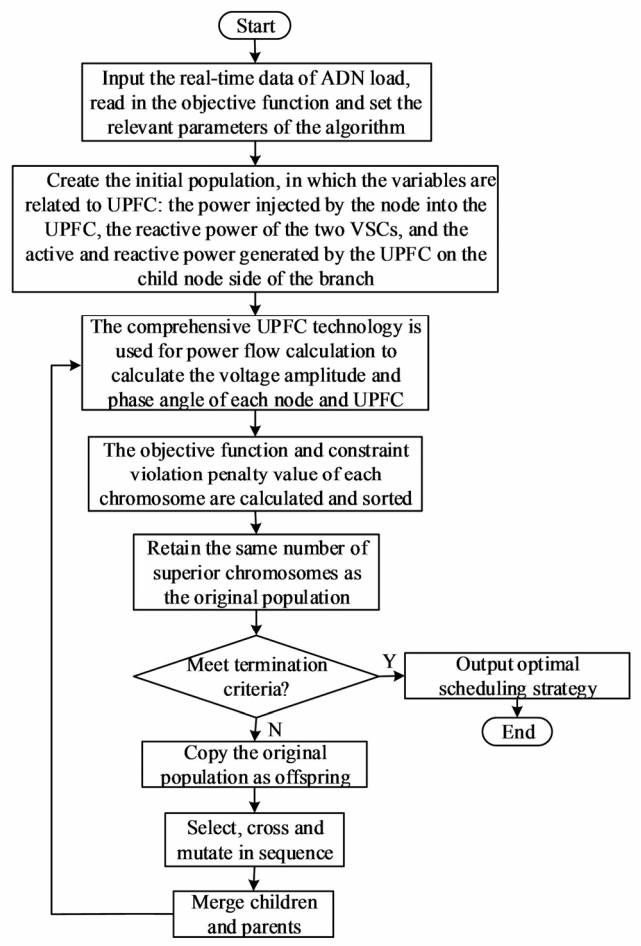

Fig.3 Specific process of optimal power flow calculation based on comprehensive technology

problem. Let Node 1 be a balanced node with a voltage amplitude of 12.95 kV and an angle of 0 degrees. The genetic algorithm is used to solve the optimal power flow. Since the voltage at the series side of the transformer of UPFC is on the ADN branch, the original power flow algorithm is no longer applicable. Therefore, the power flow equation and Newton Jacobian matrix are improved. Substitute equation (5) into equations (15) and (16) and deform:

$$P_{ij1} = r_{ij}U_jU_i[(g_{ij}\cos\rho_{ij} - b_{ij}\sin\rho_{ij})\cos\theta_{ij} - (g_{ij}\sin\rho_{ij} + b_{ij}\cos\rho_{ij})\sin\theta_{ij}] \quad (55)$$

$$Q_{ij1} = -r_{ij}U_iU_j[(g_{ij}\cos\rho_{ij} - b_{ij}\sin\rho_{ij})\sin\theta_{ij} + (g_{ij}\sin\rho_{ij} + b_{ij}\cos\rho_{ij})\cos\theta_{ij}] \quad (56)$$

When j is the parent node of i, equations (55) and (56) become:

$$P_{ji1} = r_{ji}U_iU_j[(g_{ij}\cos\rho_{ji} - b_{ij}\sin\rho_{ji})\cos\theta_{ij} + (g_{ij}\sin\rho_{ji} + b_{ij}\cos\rho_{ji})\sin\theta_{ij}] \quad (57)$$

$$Q_{ji1} = r_{ji}U_iU_j[(g_{ij}\cos\rho_{ji} - b_{ij}\sin\rho_{ji})\sin\theta_{ij} - (g_{ij}\sin\rho_{ji} + b_{ij}\cos\rho_{ji})\cos\theta_{ij}] \quad (58)$$

In order to express the Jacobian matrix conveniently, four equivalent variables G_{ji}^{U}, B_{ji}^{U}, G_i^{UP} and B_i^{UP} are introduced. G_{ji}^{U} and B_{ji}^{U} are the variables of equations (57) and (58), ordering:

$$G_{ji}^{\mathrm{U}} = \sum_{j\in M(i)} r_{ji}(g_{ij}\cos\rho_{ji} - b_{ij}\sin\rho_{ji}) \quad (59)$$

$$B_{ji}^{\mathrm{U}} = \sum_{j\in M(i)} r_{ji}(g_{ij}\sin\rho_{ji} + b_{ij}\cos\rho_{ji}) \quad (60)$$

where G_{ji}^{U} and B_{ji}^{U} are mutual admittance elements generated by UPFC on branch ji, and node j is the parent node of i. If node j is not the parent node of i, this item is 0. G_i^{UP} and B_i^{UP} are the variables of equations (13) and (14), ordering:

$$G_i^{\mathrm{UP}} = \sum_{j\in N(i)} r_{ij}(g_{ij}\cos\rho_{ij} - b_{ij}\sin\rho_{ij}) \quad (61)$$

$$B_i^{\mathrm{UP}} = \sum_{j\in N(i)} r_{ij}(g_{ij}\sin\rho_{ij} + b_{ij}\cos\rho_{ij}) \quad (62)$$

where G_i^{UP} and B_i^{UP} are the self admittance elements generated by UPFC on branch ji, and node j is a child node of i. If node j is not the child node of i, this item is 0. Replace equations (59)-(62) into equation (45) to obtain the power flow equation model considering UPFC which is consistent with the original power flow equation form:

$$\begin{cases} P_i = U_i\sum_{j\in\Omega(i)} U_j[(G_{ij} - G_{ji}^{\mathrm{U}})\cos\theta_{ij} + (B_{ij} - B_{ji}^{\mathrm{U}})\sin\theta_{ij}] \\ \qquad + (G_{ii} + G_i^{\mathrm{UP}})U_i^2 \\ Q_i = U_i\sum_{j\in\Omega(i)} U_j[(G_{ij} - G_{ji}^{\mathrm{U}})\sin\theta_{ij} - (B_{ij} - B_{ji}^{\mathrm{U}})\cos\theta_{ij}] \\ \qquad - (B_{ii} + B_i^{\mathrm{UP}})U_i^2 \end{cases} \quad (63)$$

In the iterative process of genetic algorithm, after generating the voltage regulation radius and phase initial value generated by UPFC on the branch, the admittance matrix generated by UPFC in the improved power flow equation is a constant, and its form is consistent with that of the original power flow equation. The Jacobian matrix is transformed into:

$$H_{ij} = -U_iU_j[(G_{ij} - G_{ji}^{\mathrm{U}})\sin\theta_{ij} - (B_{ij} - B_{ji}^{\mathrm{U}})\cos\theta_{ij}] \quad (64)$$

$$H_{ii} = U_i\sum_{j\in\Omega(i)} U_j[(G_{ij} - G_{ji}^{\mathrm{U}})\sin\theta_{ij} - (B_{ij} - B_{ji}^{\mathrm{U}})\cos\theta_{ij}] \quad (65)$$

$$N_{ij} = -U_iU_j[(G_{ij} - G_{ji}^{\mathrm{U}})\cos\theta_{ij} + (B_{ij} - B_{ji}^{\mathrm{U}})\sin\theta_{ij}] \quad (66)$$

$$N_{ii} = -U_i\sum_{j\in\Omega(i)} U_j[(G_{ij} - G_{ji}^{\mathrm{U}})\cos\theta_{ij} + (B_{ij} - B_{ji}^{\mathrm{U}})\sin\theta_{ij}]$$

$$-2(G_{ii}+G_i^{\mathrm{UP}})U_i^2 \tag{67}$$

$$K_{ij}=U_iU_j[(G_{ij}-G_{ji}^{\mathrm{U}})\cos\theta_{ij}+(B_{ij}-B_{ji}^{\mathrm{U}})\sin\theta_{ij}] \tag{68}$$

$$K_{ii}=-U_i\sum_{j\in\Omega(i)}U_j[(G_{ij}-G_{ji}^{\mathrm{U}})\cos\theta_{ij}+(B_{ij}-B_{ji}^{\mathrm{U}})\sin\theta_{ij}] \tag{69}$$

$$L_{ij}=-U_iU_j[(G_{ij}-G_{ji}^{\mathrm{U}})\sin\theta_{ij}-(B_{ij}-B_{ji}^{\mathrm{U}})\cos\theta_{ij}] \tag{70}$$

$$L_{ii}=-U_i\sum_{j\in\Omega(i)}U_j[(G_{ij}-G_{ji}^{\mathrm{U}})\sin\theta_{ij}-(B_{ij}-B_{ji}^{\mathrm{U}})\cos\theta_{ij}]+2(B_{ii}+B_i^{\mathrm{UP}})U_i^2 \tag{71}$$

where H, N, K and L are Jacobian matrix elements. The specific flow of optimal power flow calculation of improved comprehensive technology is shown in Fig. 4.

This method can directly optimize UPFC control parameters, voltage regulation radius and phase angle, through intelligent algorithm to reduce the search space. X can be solved through improved power flow calculation without adding the solution dimension of Newton power flow calculation. When the number and location of UPFC change, only the corresponding elements in Jacobian matrix need to be modified for power flow calculation, which reduces the burden of staff. Finally, it can be described as the solution of the following equations:

$$F(X)=0 \tag{72}$$

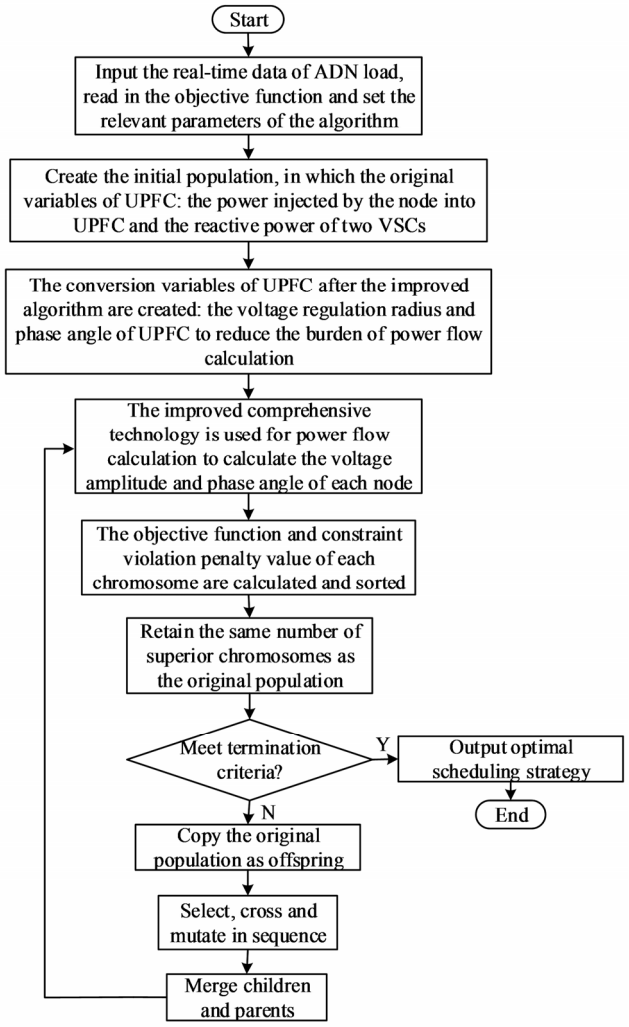

Fig.4 Specific process of optimal power flow calculation based on improved comprehensive technology

4 Example Verification

Based on the simulation environment i7-9750CPU, 8 GB memory notebook and MATLAB R2016b, this paper analyzes the IEEE33 node ADN system as an example. Its network structure is shown in Fig. 5. The system includes 33 branches, and it operates radially. The active power of user's power load is 6 530 kW. The reactive power of user's power load is 4 892.7 kvar. The period length is 1 h. One MT is connected to nodes 5, 10 and 28, respectively, and its parameters are shown in Table 1. The voltage level is 12.66 kV, and the upper and lower limits of node voltage are 1.05 and 0.95 times of the voltage level respectively. The load connected to nodes 7, 20 and 33 can be reduced. The upper limit of reduction is 200 kW. The upper limit of interactive active power with the superior power grid is 100 kW, the upper limit of interactive reactive power with the superior power grid is 100 kvar. The power sales price is 0.45 CNY/kW·h, interactive power price with superior power grid λ_{P0} is 0.74 CNY/kW·h, and load reduction price λ_{CUT} is 0.6 CNY/kW·h. UPFC is installed on branch 89, and its parameters are shown in Table 2.

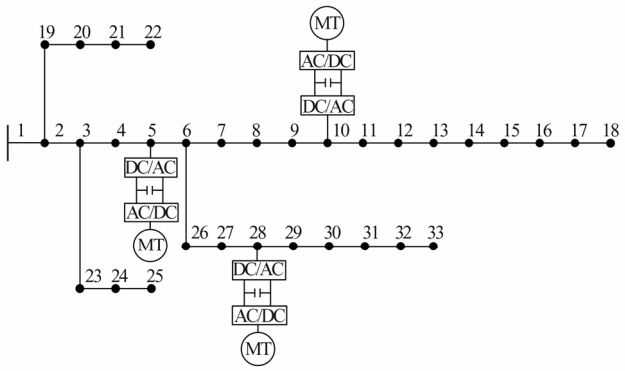

Fig.5 Active distribution network structure

Table 1 Parameters of MT model

Node	$P_{\min}$/ kW	$P_{\max}$ /kW	$S_{\max}$ /kV·A	λ_{MT}/ (CNY/MW·h)	VSC loss factor
5	200	3 100	3 200	150	0.01
10	200	2 400	2 500	150	0.01
28	200	2400	2500	150	0.01

Table 2 Parameters of UPFC model

Parameter	Value
Equivalent resistance of series and parallel side transformer/Ω	0.04
Rated voltage of series and parallel side transformer/kV	20.00
No load loss of series and parallel side transformers/kW	0.43
Voltage ratio between the valve side and the grid of the UPFC series side transformer	3.00
Maximum voltage regulation radius / times	0.90
VSC reactive upper limit/kvar	400.00
VSC lower reactive power limit/kvar	0.00
VSC maximum capacity/kW	1200.00
VSC loss factor	0.01

4.1 Analysis of Optimization Algorithm in This Paper

When UPFC is not included, the interactive active power with the superior power grid is 0 kW, the load reduction of nodes 7, 20 and 33 are 0, 200 and 11.27 kW respectively, and the minimum optimized operation cost is 1240.37 CNY.

Set initial value: the non UPFC variable takes the optimized value when excluding and UPFC, and the UPFC variable takes 0. After considering the optimization control of UPFC, the comparison of optimization results with and without UPFC is shown in Table 3. The optimization control value of UPFC is shown in Table 4, and the minimum operation cost is 1 180.6 CNY. UPFC reduces the operation cost by 59.77 CNY.

Table 3 Comparison of optimization results with / without UPFC

Item	Without UPFC	With UPFC
Interaction with superior power grid/kW	0.00	0.00
Load reduction/kW	211.27	73.09
Network loss/kW	113.63	109.33
MT power generation/kW	6 595.05	6 737.33
VSC loss of MT/kW	162.70	159.88
UPFC loss/kW	0.00	11.14

Table 4 UPFC optimized control value

Branch	r_{ij} /times	ρ_{ij} /rad	$P_{r,ij}$ /kW	$Q_{VSC1,ij}$ /kvar	$Q_{VSC2,ij}$ /kvar
89	0.056 8	4.676	367.422	312.931	249.726

Considering the optimal control of UPFC, UPFC reduces the network loss by 4.3 kW. Although the VSC of MT and UPFC losses increase by 8.32 kW, the reactive support of UPFC reduces the reactive output of MT, enabling MT to use this part of capacity to generate active power, thus reducing the load reduction by 138.18 kW. UPFC improves the operation network loss to a certain extent and provides reactive power support for the system.

4.2 Algorithm Comparison and Analysis

UPFC power flow optimization is based on genetic algorithm. The power flow algorithm uses comprehensive UPFC technology and improved comprehensive UPFC technology in this paper. The comparison algorithm, which uses comprehensive UPFC technology, needs to set the active and reactive variables generated by UPFC on the sub node side of the branch with the upper and lower limits of 10 000 and −10 000. The voltage amplitude and phase angle of UPFC are obtained through the power flow calculation.

Set the same better initial value: the non UPFC variable takes the value meeting the power flow, and the UPFC variable takes 0. The running time of each iteration of the two algorithms in Section 3 is shown in Fig. 6. The improved algorithm can directly use the voltage regulation radius and phase angle for power flow calculation without adding the dimension of Jacobian matrix. Therefore, the operation time of each iteration in this paper is lower than that of the original algorithm, and the average operation time of each iteration is reduced by 0.25 s; Because the optimization range of UPFC parameter variables in the improved algorithm is much smaller than that in the original algorithm, the improved algorithm can find the better UPFC parameters in the second iteration to reduce the power flow calculation

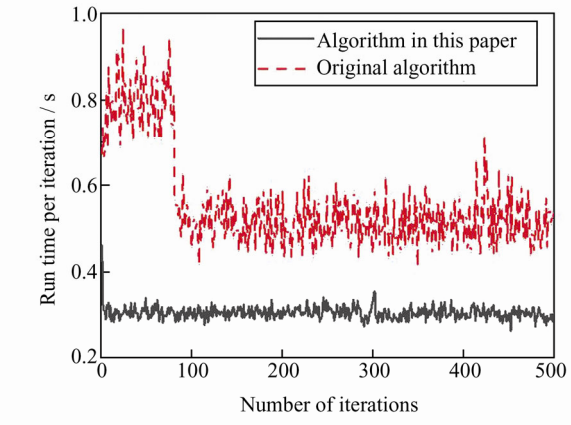

Fig.6 The running time curves of each iteration for the two algorithms

time, while the original algorithm can find the better UPFC related parameters only in the 81st iteration. The variation range of UPFC parameters in each iteration of the improved algorithm is small. After finding the better UPFC parameters, the fluctuation of calculation time is small.

The convergence comparison curve of the two algorithms after 20-500 iterations is shown in Fig. 7. It has tended to converge when the two algorithms are iterated 400 times. The running times of the two algorithms in this paper and comparison are 2.02 and 3.79 min, respectively. The optimization objective of the comparison algorithm is 1 292.1 CNY, which is 111.5 CNY higher than the optimization result in this paper, and the optimization value after improvement is reduced by 8.6%. Therefore, the proposed optimization algorithm has better convergence effect and shorter optimization time.

In order to further verify the effectiveness of the proposed algorithm and consider the influence of the number of UPFC on the two algorithms, the Monte Carlo

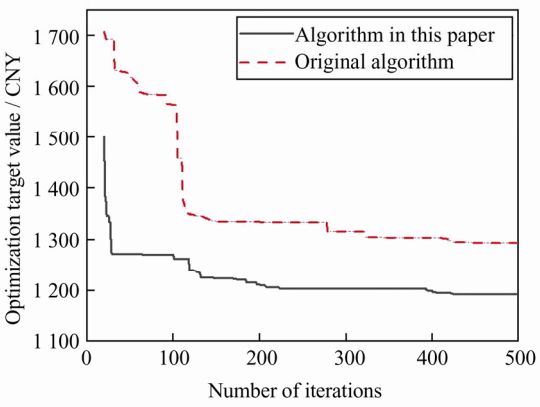

Fig.7 Convergence curves of two optimization algorithms

method is used to calculate 50 times for three scenarios. Scenario 1: UPFC is installed on branch 89. Scenario 2: UPFC is installed on branches 89 and 45. Scenario 3: UPFC is installed on branches 89, 45 and 23. The box diagram is used to describe the distribution of 50 solutions in each of the three scenarios, as shown in Fig. 8.

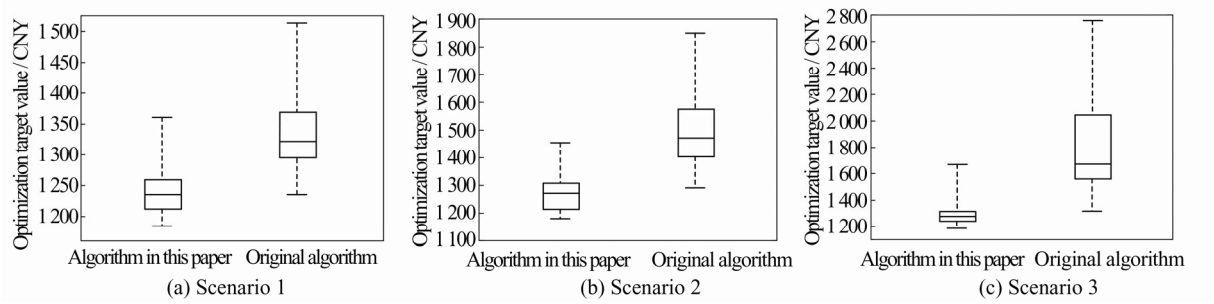

Fig.8 Comparison of fifty experimental results between the two algorithms

As can be seen from Fig. 8, the randomly generated initial population will make it difficult for the algorithm to converge to the optimal solution, and there are large penalty function values. However, the improved algorithm in this paper has better solution accuracy as a whole. Compared with the original algorithm, it has a lower median and the obtained solution is more concentrated. Therefore, the algorithm in this paper has a greater probability to obtain a better solution than the original algorithm. In addition, with the increase of the number of UPFC, the search space difference between the original algorithm and the algorithm in this paper will increase exponentially. Therefore, the median of the original algorithm is higher and higher, and the obtained solutions are more and more scattered. However, the algorithm in this paper plays a stable role, the median remains between 1 200 and 1 300 CNY, and 75% of the solutions are concentrated below 1 300 CNY.

5 Conclusion

By improving the comprehensive UPFC technology, the dimension of Jacobian matrix is not increased in the Newton power flow calculation with UPFC, and the UPFC control parameters can be directly optimized in the intelligent algorithm. Through theoretical and simulation analysis, the following conclusions can be drawn:

1) The proposed calculation method can realize power flow optimization of power system, develop the power regulation potential of UPFC and expand the types of ADN control resources on the basis of connecting with traditional UPFC.

2) The self-admittance and mutual admittance elements generated by UPFC are introduced into Jacobian matrix without adding the dimension of power flow calculation. Combined with intelligent optimization, it has

better convergence and operation speed than comprehensive UPFC technology.

3) Setting UPFC voltage regulation radius and phase angle optimization variables can reduce the search space and improve the convergence, and retain the better UPFC parameters as the initial value of power flow calculation in each iteration, so as to improve the calculation speed.

The solution of the optimal value in this method is affected by the initial value, and the better value satisfying the power flow should be selected. In addition, with the development of distributed generation, a new UPFC based on DC side energy storage has emerged[27]. The access of energy storage makes the relationship between UPFC variables more complex and improves the difficulty of optimization. In the future, the optimal power flow calculation of the new UPFC based on DC side energy storage can be studied to further tap the regulation potential of UPFC.

References

[1] Teng D Y, Teng H, Liu X, *et al*. Multi-objective reactive power optimization of the distribution network considering a large number of DGs access [J]. *Electrical Measurement & Instrumentation*, 2019, **56**(13): 39-44(Ch).

[2] Zhang A X, Song S Z, Gao Y, *et al*. Hierarchical distributed coordinated control of active distribution network including energy interconnection micro grid [J]. *Power System Protection and Control*, 2019, **47**(19): 131-138(Ch).

[3] Xiao Z F, Xin P Z, Liu Z G, *et al*. An overview of planning technology for active distribution network under the situation of ubiquitous power Internet of things [J]. *Power System Protection and Control*, 2020, **48** (3): 43-48(Ch).

[4] Yin Y Y. Power flow monitoring technology for photovoltaic power distribution network monitoring system [J]. *Automation and instrumentation*, 2018 (12): 169-172(Ch).

[5] Liu D, Zhang H, Wang J C. Review on the state of the art of active distribution network technology research [J]. *Electric Power Engineering Technology*, 2017, **36**(4): 2-7 + 20(Ch).

[6] Zhang J, Huang S F, Li Y F. Analysis of the influence of UPFC on distance protection and the corresponding improved scheme [EB/OL]. [2021-06-26]. *http://infcn.lib. ctgu. edu. cn*: 80/*rwt*/*CNKI*/*http*/*NNYHGLUDN3WXTLUPMW4A*/*kcms*/*detail*/23.1202.TH.20200721.0859.002.*html*(Ch).

[7] Qi W C, Cai H, Xue J L, *et al*. Research of the effect of 500 kV UPFC on improving system stability of HVDC feeding power grid [J]. *Electrical Measurement & Instrumentation*, 2018, **55**(18): 115-119(Ch).

[8] Wu X, Wang L, Chen X, *et al*. Comparative research on UPFC and IPFC enhancing transmission capability of a power system [J]. *Power System Protection and Control*, 2020, **48** (9): 128-134(Ch).

[9] Wu W C, Tian Z, Zhang B M. An exact linearization method for OLTC of transformer in branch flow model[J]. *IEEE Transactions on Power Systems*, 2017, **32**(3): 2475-2476.

[10] Ouyang C, Wei Z N, Sun G Q. Optimal power flow with UPFC based on tree growth algorithm [J]. *Electric Power Engineering Technology*, 2020, **39**(3): 84-91(Ch).

[11] Sun R, Zhu Z R, Wei Z N, *et al*. Multi-Objective and multi-stage reactive power optimization algorithm for power system considering UPFC [J]. *Electric Power Engineering Technology*, 2020, **39** (1): 76-85(Ch).

[12] Liu S S, Zhou T, Zhang N Y, *et al*. Optimal power flows with UPFC and minimum voltage stability constraint [J]. *Electric Power Engineering Technology*, 2019, **38**(1): 62-66(Ch).

[13] Sayed M A, Takeshita T. All nodes voltage regulation and line loss minimization in loop distribution systems using UPFC [J]. *IEEE Trans on Power Electronics*, 2011, **26**(6): 1694-1703.

[14] Liu J L. *Research on Power Flow Regulation Characteristics and Control Strategy of UPFC* [D]. Hangzhou: Zhejiang University, 2020(Ch).

[15] Kamel S, Jurado F, Lopes J A P. Comparison of various UPFC models for power flow control [J]. *Electric Power Systems Research*, 2015, **121**: 243-251.

[16] Jian Y, Zheng X. Power flow calculation methods for power systems with novel structure UPFC [J]. *Applied Sciences*, 2020, **10**(15): 5121-5128.

[17] Li S H, Wang T, Xue J, *et al*. Control of active power loops in power system with UPFC based on power flow sensitivity [J]. *Power System Technology*, 2018, **42**(11): 3768-3775 (Ch).

[18] Wu Z H. *Research on Power System Optimal Power Flow with Considering Unified Power Flow Controller* [D]. Shenyang: Shenyang University of Technology, 2013(Ch).

[19] Zhang X, Li R, Ma T, *et al*. Stackelberg game and greedy strategy based optimal dispatch of active distribution network with electric vehicles [J]. *Electric Power Automation Equipment*, 2020, **40**(4): 103-110(Ch).

[20] Zhao J B, Wei Z N, Zhu Z R, *et al*. Reactive power optimization algorithm considering device action times and UPFC[J]. *Electric Power Automation Equipment*, 2020, **40**(12): 179-187(Ch).

[21] Xu C B, Yang X D, Zhang Y B, *et al*. Stochastic operation optimization method for active distribution network with soft open point considering risk management and control [J]. *Automation of Electric Power Systems*, 2021, **45**(11): 68-

76(Ch).

[22] Hua L L, Huang W, Ge L J, *et al*. Bi-level optimal dispatch model for active distribution network with demand response [J]. *Electric Power Construction*, 2018, **39**(9): 112-119(Ch).

[23] Cheng Z L. *Research on the Power Flow Calculation and Optimized Operation of Distribution Network with Distributed Generations* [D]. Chengdu: Southwest Jiaotong University, 2011(Ch).

[24] Li C, Miao S H, Sheng W X, *et al*. Optimization operation strategy of active distribution network considering dynamic network reconfiguration [J]. *Transactions of China Electrotechnical Society*, 2019, **34**(18): 3909-3919(Ch).

[25] Li Z K, Cui J, Lu Q, *et al*. Rolling optimal scheduling of active distribution network based on sequential dynamic constraints [J]. *Automation of Electric Power Systems*, 2019, **43**(16): 17-24(Ch).

[26] Fuerte-Esquivel C R, Acha E. Unified power flow controller: A critical comparison of Newton-Raphson UPFC algorithms in power flow studies [J]. *IEE Proc Gener Transm Distrib*, 1997, **144**(5): 437-444.

[27] Wang Q, Yi J, Liu L P, *et al*. Optimal design of a novel unified power flow controller incorporated with a battery energy storage system at DC side [J]. *Proceedings of the CSEE*, 2015, **35**(17): 4371-4378(Ch).

□